VANADIUM OXIDES SUPPORTED ON HYDROTALCITE-TYPE PRECURSORS: THE EFFECT OF ACID-BASE PROPERTIES ON THE OXIDATION OF ISOPROPANOL

D. M. Meira[1], G. G. Cortez[1,*], W. R. Monteiro[2] and J. A. J. Rodrigues[2]

[1]Laboratório de Catálise II, Departamento de Engenharia Química, Faculdade de Engenharia Química de Lorena,
Phone: +(55) (12) 3159-5105, Fax: +(55) (12) 3153-3224,
Rod. Itajuba-Lorena, Km 74,5, Campus I, CEP 12600-000, Lorena, SP - Brazil.
E-mail: cortez@dequi.faenquil.br
[2]Laboratório Associado de Combustão e Propulsão, Instituto Nacional de Pesquisas Espaciais,
Phone: +(55) (12) 3186-9259, Fax: +(55) 3101-1992,
Rod. Presidente Dutra, Km 40, CEP 12630-000, Cachoeira Paulista, SP - Brazil.
E-mail: jajr@lcp.inpe.br

Abstract - Vanadium oxide supported on hydrotalcite-type precursors was studied in the oxidation of isopropanol. Hydrotalcites with different y = Mg/Al ratios were synthesized by the method of coprecipitation nitrates of Mg and Al cations with K_2CO_3 as precipitant. The decomposition of these hydrotalcite precursors at 450°C yielded homogeneous MgyAlOx mixed oxides that contain the Al^{+3} cations totally incorporated into the MgO framework. The materials were characterized by chemical analysis, BET superficial area, X-ray diffraction, temperature-programmed reduction (TPR) and the reaction of isopropanol, a probe molecule used to evaluate the acid-base properties. The results of TPR showed that the reducibility of V^{+5} decreased with the increase in magnesium loading in catalysts. The X-ray diffraction patterns of Al-rich hydrotalcite precursors showed the presence of crystalline phases of brucite and gibbsite. It was shown that chemical composition, texture, acid-base properties of the active sites and also Mg/Al ratio strongly affect the formation of the products in the oxidation of isopropanol. The Al-rich catalysts were much more active than the Mg-rich ones, converting isopropanol mainly to propylene.
Keywords: Mixed oxides; Hydrotalcites; Isopropanol; V-Mg-Al catalysts.

INTRODUCTION

Hydrotalcite-type clays, $Mg_6Al_2(OH)_{16}CO_3.4H_2O$, and many other related minerals are basic solids with large surface areas (Miyata, 1983). Synthetic hydrotalcite-like layered double hydroxide (LDHs) compounds are mixed metal hydroxides with the general formula $[M_{1-x}^{+2}M_x^{+3}(OH)_2][A^{-m}]_{x/m}.nH_2O$ where M^{+2} and M^{+3} represent divalent and trivalent cations at the octahedral sites within the hydroxyl layers, x is equal to the ratio of $M^{+3}/(M^{+2} + M^{+3})$ with a value varying in the range of 0.17 to 0.50 and A^{-m} is an exchangeable interlayer anion. LDHs have attracted much attention in recent years as catalyst precursors and catalyst support due to the ability of these materials to accommodate a large variety of divalent and trivalent cations and the formation of well-dispersed mixed oxides upon controlled thermal decomposition (Cavani et al., 1991). The catalytic properties of the hydrotalcite-derived mixed oxides

---

*To whom correspondence should be addressed

largely depend on the activation procedure (Tichit et al., 1997).

Catalysts containing vanadium as the main component are among the most extensively studied for oxidative dehydrogenation (ODH) processes (Mamedov and Carberán, 1995). In particular, much attention has been given to the V-Mg-O mixed system, which has proved to be one of the most active and selective in the ODH of short-chain paraffins to the corresponding olefins (López Nieto et al., 1999). Vanadate-intercalated LDHs have a possible application as precursors to catalysts for the selective oxidation of short-chain paraffins (Dula et al., 2002).

The transformation of isopropanol is a widely used test reaction for characterizing both the acidic and basic properties of solids (Deepakand and Wachs, 2002). The isopropanol reaction on solid catalysts occurs through two pathways: dehydration, which is generally catalyzed by the acidic sites or both acidic and basic sites, and dehydrogenation, which is catalyzed by basic sites.

In the present work, Mg-Al hydrotalcite precursors with different Mg/Al molar ratios were synthesized by the coprecipitation method. The effect of interlayer doping with vanadium on the catalytic properties of mixed oxide phases obtained upon calcination of corresponding LDH precursors was studied for the isopropanol reaction, a probe molecule used to evaluate the acid-basic properties of the catalyst. The samples were also characterized by chemical analysis, BET surface area, temperature-programmed reduction (TPR) and X-ray diffraction (XRD).

EXPERIMENTAL

The hydrotalcite-type precursors were prepared by continuous coprecipitation at constant pH and temperature. This method comprises the simultaneous addition of an aqueous solution of magnesium ($Mg(NO_3)_2.6H_2O$) and aluminum ($Al(NO_3)_3.9H_2O$) with theoretical Mg/Al atomic ratios in the range of 0.5 to 1.0 and K_2CO_3 (1.5 M) as precipitant in the 150 mL continuously stirred reactor (Figure 1) under vigorous stirring at constant pH = 10 and at a temperature of 55°C. After addition of reagents, the gel obtained was aged at 40°C for 18 h under gentle stirring. The material was cooled to room temperature, filtered and washed with a large amount of deionized water up to a pH of 7 for complete removal of K^+ and dried at 90°C for 12 h.
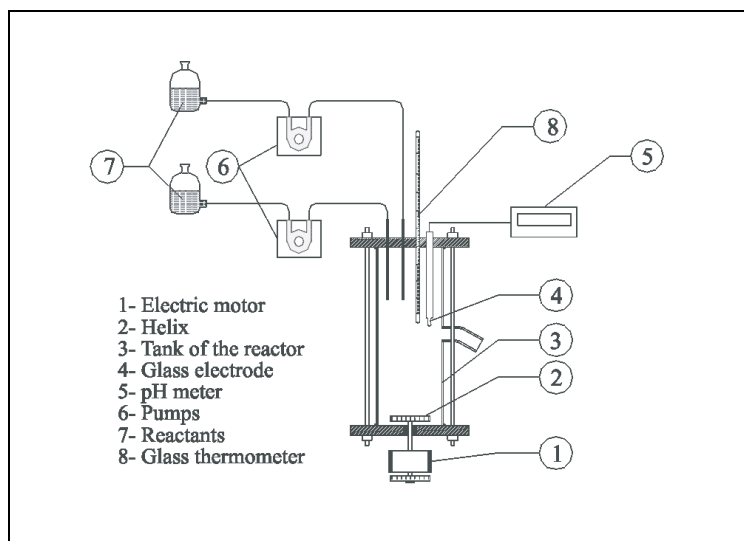

Figure 1: Continuously stirred reactor

A series of vanadium-containing catalysts with V_2O_5 loadings of 17 wt% were prepared by a single impregnation of the dry LDH precursors with aqueous solution containing ammonium metavanadate (Merck) at a temperature of 70°C. Then the solids were dried at 90°C for 18 h and calcined at 450°C for 4 h. Samples are labeled V/MgyAl, where y is Mg/Al atomic ratios of 0.5, 0.89 and 1.0.

The elemental composition of the samples was determined by atomic absorption spectroscopy (AAS). The samples were digested with a mixture of HNO_3 and HF acids. The measurements were obtained by the method of addition of standard solution using Perkin-Elmer Analyst equipment.

BET surface areas were measured with a Quantachrome NOVA 1000 instrument by adsorption

of nitrogen at – 196°C on 150 mg of samples, previously degassed at 200°C in high vacuum for 2 h.

XRD patterns were obtained with a SEISERT Isodebyeflex 1001 diffractometer operated at 40 kV and 30 mA using Ni-filtered CuKα radiation (λ = 0.15418 nm). The samples in powder form were analyzed without previous treatment after deposition on a quartz sample holder. The identification of crystalline phases was based on references from the ASTM files.

Temperature-programmed reduction (TPR) results were obtained in a Quantachrome Chembet-3000 apparatus loaded with 25 mg of catalyst. The samples were first treated in helium at a temperature of 150°C for 1 h. The samples were cooled to room temperature and a mixture of H_2/N_2 was subsequently added to the sample (H_2/N_2 molar ratio of 0.15 and a total flow of 40 mL/min) and heated at a rate of 10°C/min to a final temperature of 900^0C.

The catalyst test of isopropanol transformation (Figure 2) was realized in a fixed-bed quartz tubular reactor (i.d. 10 mm, length 400 mm) operated at atmospheric pressure and temperature in the range of 170 to 290°C. The reactor was equipped with a coaxial thermocouple for catalytic bed temperature profiling. The isopropanol (99.7%, Merck) was injected into the feeding pipe with the aid of a Thermo Separation Product Spectra P100 pump, at a flow rate of 0.05 cm^3/min and diluted in a mixture of He and O_2 (molar ratio of 3/1) at a flow rate of 74 cm^3/min. Reactants and reaction products were analyzed with a on-line gas chromatograph (VARIAN 3350 equipped with a thermal conductivity detector (TCD)). A Carbowax 20 M on Chromosorb-W column was used for separation of products. The catalyst mass was 100 mg, the particle size was 0.5 to 0.85 mm and the time of contact was 2.4 g.h/mol_{Isop}. The conversion was calculated from the reaction product on the basis of the carbon balance: the total molar amount of carbon in the effluent was assumed to be equal to the molar amount of carbon in the isopropanol fed into the reactor.
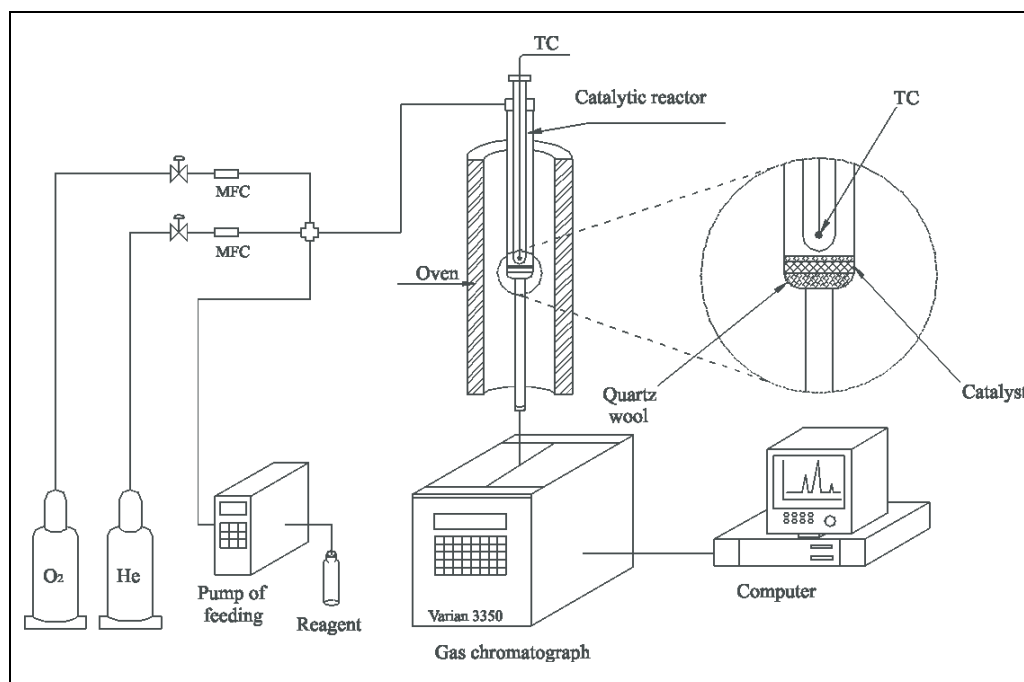

Figure 2: Scheme of the catalytic system. Notes: MFC, mass flow controller; TC, thermocouple. Gas sources: He, helium grade 5.0; O_2, oxygen grade 6.0.

RESULTS AND DISCUSSION

The chemical composition and BET specific surface area (Sg) of the catalysts are shown in Table 1.

Elemental chemical analysis data for Mg and Al were similar to those expected from the initial concentrations of the solutions used during synthesis, suggesting complete precipitation of Mg and Al salts during synthesis. The potassium content in all the mixed oxides was below 0.1 wt%, which confirms that potassium ions were effectively removed by washing of the precipitated precursors. The vanadium in all the catalysts was close to the nominal value. The BET specific surface area varies independent of the V_2O_5 content.

Table 1: Chemical composition and specific surface areas for the samples studied.

Sample	R* (nominal)	Chemical analysis by AAS				Sg ($m^2 \cdot g^{-1}$)
		R* (molar)	Mg (wt%)	Al (wt%)	V_2O_5 (wt%)	
V/Mg$_{1.0}$Al	0.50	0.43	15.6	11.7	18.1	99
V/Mg$_{0.89}$Al	0.53	0.54	11.8	13.8	15.6	105
V/Mg$_{0.50}$Al	0.67	0.66	8.2	15.6	16.3	128

(*) R = Al/(Al + Mg) ratio molar

Figures 3, 4 and 5 show the XRD patterns of the precursors dried at 90°C and catalyst calcined at 450°C with different molar compositions, defined as R = Al/(Mg+Al). XRD patterns for Mg-Al precursors dried at 90°C, as can be observed in Figure 3, showed that all samples contained a phase crystalline-type hydrotalcite. The precursors with R = 0.53 and R = 0.63 had the gibbsite (Al(OH)$_3$) and brucite (Mg(OH)$_2$) phases. The intensity of the diffraction lines increases with aluminum content in the precursor. The intensities of the peaks were compared with the theoretical values obtained from the files (ASTM). The variation in the intensity of the hydrotalcite peaks is related with the lattice parameter a. The parameter a values decreased linearly (following Vegard's law) with the increase in Al content from R = 0.5 (a = 3.08Å), R = 0.53 (a = 3.06Å) and R = 0.67 (a = 3.04Å). This variation in parameter a value was attributed to the substitution of the larger Mg^{+2} cations by the smaller Al^{+3} cations in the structure of the hydrotalcite. Díez et al. (2003) reported the same phases and they found that the value of the lattice parameter decreases when the amount of Al in the precursor increases from R = 0.10 (a = 3.132Å) to R = 0.67 (a = 3.020Å).

Figure 4 illustrates the XRD patterns of the three precursors dried at 90°C that were impregnated with ammonium metavanadate.
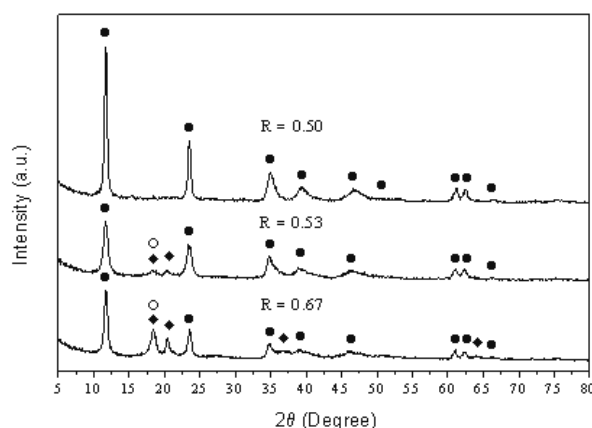

Figure 3: XRD patterns of precursors dried at 90°C (●) hydrotalcite, (◆) gibbsite and (○) brucite.
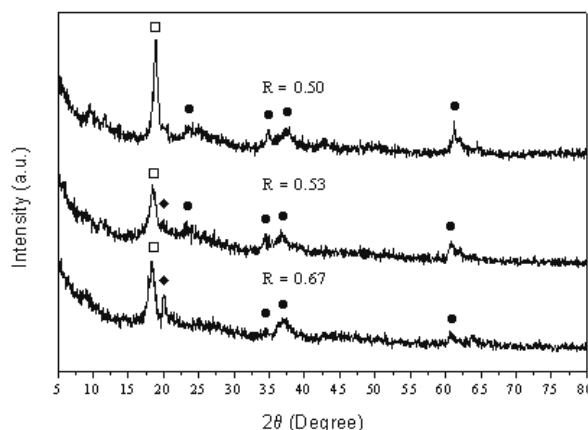

Figure 4: XRD patterns of V-LDH precursors (●) hydrotalcite, (◆) gibbsite and (□) unidentified phase.

An intense peak was observed in the three samples at $2\theta = 18.32°$ (R = 0.50), $2\theta = 18.47°$ (R = 0.53) and $2\theta = 18.89°$ (R = 0.67). Other less intense peaks correspond to the phase gibbsite ($2\theta \approx 20.04°$) and Mg-Al hydrotalcite ($2\theta \approx 24.12°$, 35.21°, 39.01° and 61.21°). No peaks due to V_2O_5 crystalline are seen in any of the samples. Bhattacharyya et al. (1995) prepared oligovanadate-pillared hydrotalcite-type materials. The solid obtained with pH in the range of 7.0-8.5 showed an XRD pattern characteristic of a hydrotalcite-type structure with a more intense peak at $2\theta = 18.50°$. They found that the species oligovanadate of the precursor was $V_4O_{12}^{-4}$ anions, found in the interlayer of the structure of the hydrotalcite. Dinka et al. (1998) considered that the d_{001} spacing value of the decavanadate ($V_{10}O_{28}^{-6}$) intercalated LDHs was 9.9Å. Other authors (Dula et al., 2002) introduced

decavanadate anions into the interlayer space of the Mg-Al precursor with hydrotalcite structure. They found a peak corresponding to the α-$Mg_2V_2O_7$ magnesium pyrovanadate phase at $2\theta \approx 18.0°$ (ASTM 39-816) in the sample calcined at 550°C. In our results obtained by XRD, the diffraction lines at $2\theta \approx$ 18.30°, 18.51° and 18.93° (Figure 2) can correspond to the $V_4O_{12}^{-4}$ anions found in the interlayer of the precursor with a hydrotalcite structure, $Mg_4Al_2(OH)_{12}(V_4O_{12})_{0.5}$ (Bhattacharyya et al., 1995).

The XRD patterns of the vanadium-containing LDHs, calcined at 450°C, are presented in Figure 5. The peaks at $2\theta = 35.10°$, 43.03° and 63.12° correspond to the MgO phase in the three samples and a small peak at $2\theta = 65.03°$ is attributed to the $MgAl_2O_4$ phase for the catalyst with R = 0.67. No peaks due to V_2O_5 crystalline are seen in any of the catalyst samples.
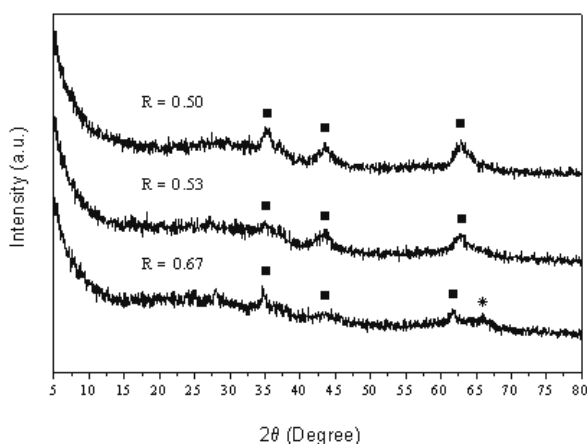

Figure 5: XRD patterns of V-LDH precursors calcined at 450°C, (■) MgO and (∗) $MgAl_2O_4$.

TPR profiles for pure V_2O_5 and catalysts are presented in Figure 6. The TPR profile using bulk V_2O_5 shows two major peaks at 663°C and 696°C and one minor reduction peak at 836°C (Figure 6-a). The peaks correspond to a reduction of $V^{+4.33}$ (first step), V^{+4} (second step) and V^{+3} (third step). The same TPR profile was obtained by Koranne et al. (1994) using the V_2O_5 bulk.

Figures 6b-6d show TPR profiles for V/Mg_yAl catalysts. The presence of a single reduction peak in the V/Mg_yAl catalysts is due to the reduction of V^{+5} to V^{+4} species. The results also showed that the maximum temperature of reduction of the vanadium increases with the increase in the amount of

magnesium in the catalyst, starting from R = 0.67 (568°C), R = 0.53 (608°C) and R = 0.50 (614°C). This increase in maximum temperature of reduction can be attributed to the formation of a larger amount of MgO phase in the catalyst, which decreases the reducibility of the vanadium species.

The results of catalytic tests for the isopropanol transformation reaction on catalysts at 270°C, 280°C and 290°C are listed in Table 2. The catalytic results were calculated in terms of the consumed amount of isopropanol per area, per time (mol. m^{-2}. min^{-1}) and per rate of formation of the products (RFP). To avoid the reduction of V^{+5} species in the catalyst, oxygen was mixed with the isopropanol.
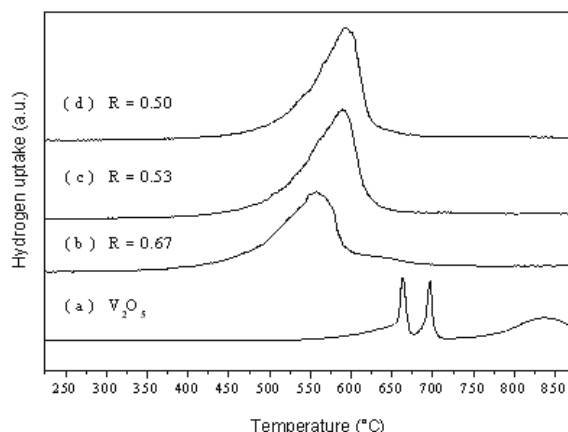
Figure 6: Temperature-programmed reduction (TPR) profiles for V/Mg$_y$Al catalysts:
(a) unsupported V$_2$O$_5$, (b) V/Mg$_{0.5}$Al, (c) V/Mg$_{0.89}$Al and (d) V/Mg$_{1.0}$Al.

Table 2: Results of catalytic tests for the reaction decomposition isopropanol reaction.

Catalyts	RFP - Rate of formation of the products ($\mu mol \; m^{-2} \; min^{-1}$)					
	Propylene			Acetone		
	270°C	280°C	290°C	270°C	280°C	290°C
V/Mg$_{1.0}$Al	1.0	18.0	40.0	30.0	29.0	21.0
V/Mg$_{0.89}$Al	9.0	29.0	38.0	26.0	23.0	21.0
V/Mg$_{0.50}$Al	38.0	40.0	41.0	12.0	11.0	9.0

The activity for isopropanol conversion showed that propylene formation increases with the increase in temperature and it is favored by the decrease in magnesium in the catalyst. On the other hand, the formation of acetone decreases with the increase in temperature and with the increase in magnesium content in the catalyst. The formation of diisopropyl ether was below 0.5% in all the catalytic tests.

Figure 7 shows the results of the catalytic test of the V/Mg$_{0.5}$Al catalyst in the isopropanol reaction versus temperature. Conversion of the isopropanol increases with increase in temperature, reaching a maximum at 290°C. Propylene formation is favored starting at a temperature of 240°C; however, the formation of acetone is inhibited above this temperature. In work mentioned previously (Wang et al., 1999), the increase in temperature favors propylene formation through dehydration of the isopropanol.
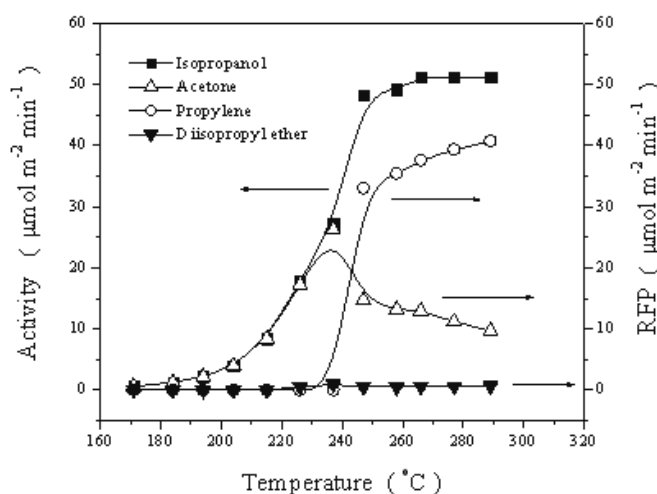

Figure 7: Catalytic activity of the V/Mg$_{0.5}$Al catalyst in the isopropanol
reaction versus temperature.

The transformation of isopropanol is frequently used as a test reaction to determine acid-base properties of oxide catalysts (Díez et al., 2003). The reaction can give as main products acetone, propylene and, to a lesser extent, diisopropyl ether. Dehydration at acid sites or concerted acid-base pair sites gives propylene and diisopropyl ether, and dehydrogenation at basic sites gives acetone. Ether formation must involve an intermolecular coupling reaction. Many contradictory interpretations concerning the mechanism of isopropanol dehydration have been presented and isopropanol transformation cannot be a simple test of acidity (Haffad et al., 2001). On the other hand, the isopropanol decomposition reaction cannot distinguish between the Lewis and Brönsted sites. The presence of species with redox properties, such as the vanadium in the catalysts synthesized in this work, can be important in the isopropanol dehydration and dehydrogenation reactions. Unsupported V_2O_5 has both Lewis and Brönsted surface acidity (Busca et al., 1989). When vanadia is supported on a metal oxide support, a decrease in the number of surface Lewis acid sites and an increase in the number of surface Brönsted acid sites has been detected (Datka et al., 1992). The decrease in Lewis acidity would be related with the coordination of the VO_X species on the metal oxide support and the increase in Brönsted acidity is due to V-OH groups of the VOH_4^{-2} and $V_2O_7H_2^{-2}$ species on the support (Ferreira and Volpe, 2002). In previous work,

Aramendía et al. (1996) reported that the isopropanol dehydratation reaction on MgO is related with Brönsted acidity. Other authors (Díez et al., 2003) reported that Al-rich Mg_yAlO_x samples (R > 5) convert isopropanol mainly to propylene via an E_2 mechanism (Scheme 1) occurring on dual Al^{+3}-O^{-2} sites. These Al-rich Mg_yAlO_x samples are mixed oxides that contain a separate quasi-amorphous Al_2O_3-like phase, which has dual Al^{+3}-O^{-2} active sites that dehydrate isopropanol to propylene at high turnover rates. In this work, the results of XRD provided evidence of the presence of the gibbsite phase in the samples with R = 0.53 and 0.67. In the calcined samples it was not possible to identify the Al_2O_3 phase, however the MgO phase was identified in all the samples and a small peak at $2\theta \approx 65°$ was attributed to the $MgAl_2O_4$ phase in the catalyst with R = 0.67. On the other hand, the increase in Al loading in the mixed oxides resulted in a larger propylene formation due to the creation of new acid sites attributed to the substitution of Mg^{+2} by Al^{+3} in the matrix of the precursor. In all the samples the vanadium loadings varied between 16 and 18 wt% of V_2O_5. The presence of vanadium on the mixed oxides favored the formation of acid sites (Lewis and Brönsted) that would participate in the formation of the propylene in all the samples. Therefore, it is important to emphasize that the lack of information about the interaction of vanadium in the structure of the hydrotalcite prevented a better interpretation of the results obtained in this study.
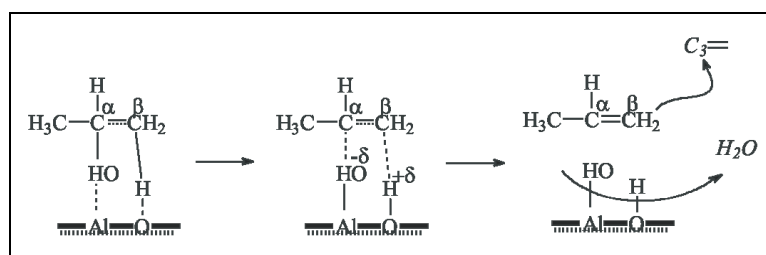
Scheme 1: Formation of propylene via E_2 mechanism occurring on dual Al^{+3}-O^{-2} sites.

CONCLUSIONS

In this work, the synthesis of the precursors with different molar ratios R = Al/(Mg+Al) in a continuous coprecipitacion reaction resulted in the formation of hydrotalcite-like materials. The increase in the composition of the aluminum in the precursor in the range of R = 0.53 to 0.67 yielded segregated phases of gibbsite and brucite in the structure of the hydrotalcite. The addition of vanadium to hydrotalcite-type precursors might have incorporated

$V_4O_{12}^{-4}$ anions in the interlayer space of the brucite-type phase. The TPR profiles showed that the growing increase in Mg loadings in the catalyst caused an increase in the maximum temperature of reduction of the vanadium species in the catalyst. This increase in the maximum temperature of reduction can be attributed to the formation of a larger amount of MgO phase in the catalyst, which decreased the reducibility of the vanadium species. In the catalytic tests for the isopropanol transformation reaction the catalyst with the largest

concentration of magnesium produced the most acetone. The highest activity in the formation of acetone in the $V/Mg_{1.0}Al$ catalyst was due to the presence of large amounts of magnesium (basic sites). Conversely, the catalyst with the largest amount of aluminum ($V/Mg_{0.5}Al$) was more selective in the formation of propylene due to a larger number of acid sites. The presence of vanadium in the catalysts favored the formation of new acid sites in the catalyst and resulted in the conversion of isopropanol to propylene.

ACKNOWLEDGMENTS

REFERENCES

Aramendía, M.A., Borau, V., Jimenez, C., Marinas, J.M., Porras, A. and Urbano, F.J., Magnesium Oxides as Basic Catalysts for Organic Processes, Journal of Catalysis, 161, 829 (1996).

ASTM file No. 39-816.

Bhattacharyya, A., Hall, D.B. and Barnes, T.J., Novel Oligovanadate-pillared Hydrotalcites, Applied Clay Science 10, 57 (1995).

Busca, G., Ramis, G. and Lorenzelli, V., On the Role of Acidity in Catalytic Oxidation, Journal of Molecular Catalysis, 50, 231 (1989).

Cavani, F., Trifiro, F. and Vaccari, A., Hydrotalcite-type Anionic Clays: Preparation, Properties and Applications, Catalysis Today, 11, 173 (1991).

Datka, J., Turek, A., Jehng, M. and Wachs, I.E., Acidic Properties of Supported Niobium Oxide Catalysts: An Infrared Spectroscopy Investigation, Journal of Catalysis, 135, 186 (1992).

Deepak, K. and Wachs, I.E., Isopropanol Oxidation by Pure Metal Oxide Catalysts: Number of Active Surface Sites and Turnover Frequencies, Applied Catalysis A: General, 237, 121 (2002).

Díez, V.K., Apestegía, C.R. and Di Cosimo, J.I., Effect of the Chemical Composition on the Catalytic Perfomance of Mg_yAO_x Catalysts for Alcohol Elimination Reactions, Journal of Catalysis, 215, 220 (2003).

Dinka, P., Prandová, K. and Hronec, M., Reaction of Methanol and n-Propanol over Hydrotalcite-like Catalysts Containing Vanadium Oxide, Applied Clay Science, 13, 467 (1998).

Dula, R., Wcislo, K., Stoch, J., Grzybowska, B., Serwicka, E.M., Kooli, F., Bahranowski, K. and Gawel, A., Layered Double Hydroxide-derived Vanadium Catalysts for Oxidative Dehydrogenation of Propane: Influence of Interlayer-doping Versus Layer-doping, Applied Catalysis A: General, 230, 281 (2002).

Ferreira, M.L. and Volpe, M., A Combined Theoretical and Experimental Study of Supported Vanadium Oxide Catalysts, Journal of Molecular Catalysis A: Chemical, 184, 349 (2002).

Haffad, D., Chambellan, A. and Lavalley, J.C., Propan-2-ol Transformation on Simple Metal Oxides TiO_2, ZrO_2 and CeO_2, Journal of Molecular Catalysis A: Chemical, 168, 153 (2001).

Koranne, M.M., Goodwin, J.G. and Marcelin, G., Characterization of Silica- and Alumina-Supported Vanadia Catalysts Using Temperature Programmed, Journal of Catalysis, 148, 369 (1994).

López Nieto, J.M., Soler, J., Concepción, P., Herguido, J., Menédez, M. and Santamaría, J., Oxidative Dehydrogenation of Alkanes over V-based Catalysts: Influence of Redox Properties on Catalytic Performance, Journal of Catalysis, 185, 324 (1999).

Mamedov, E.A. and Cortés Corberán, V., Oxidative Dehydrogenation of Lower Alkanes on Vanadium Oxide-based Catalysts. The Present State of the Art and Outlooks, Applied Catalysis A: General 127, 1 (1995).

Miyata, S., Anion-Exchange Properties of Hydrotalcite-like Compounds, Clays and Clay Minerals, 31(4), 305 (1983).

Tichit, D., Medina, F., Coq, B. and Dutartre, R., Activation under Oxidizing and Reducing Atmospheres of Ni-containing Layered Double Hydroxides, Applied Catalysis A: General, 159, 241 (1997).

Wang, J.A., Bokhimi, X., Novaro, O., Lopez, T. and Gomez, R., Effects of the Surface Structure and Experimental Parameters on the Isopropanol Decomposition Catalyzed with Sol-gel, Journal of Molecular Catalysis A: General, 145(1), 291 (1999).